Advanced Composite Materials
Publication details, including instructions for authors and subscription information:
http://www.tandfonline.com/loi/tacm20

Fatigue behavior of Nextel™ 312/Blackglas™ ceramic matrix composite with tensile and zero mean load

M. Al-Hussien [a], S. Mall [b] & J. R. Calcaterra [c]

[a] Department of Aeronautics and Astronautics, Air Force Institute of Technology, USA

[b] Materials and Manufacturing Directorate, Air Force Research Laboratory, AFIT/ENY, 2950 P.St., Bldg. 640, Wright-Patterson Air Force Base, OH 45433, USA

[c] Department of Aeronautics and Astronautics, Air Force Institute of Technology, USA

Version of record first published: 02 Apr 2012.

Adv. Composite Mater., Vol. 10, No. 1, pp. 1–15 (2001)

Fatigue behavior of Nextel™ 312/Blackglas™ ceramic matrix composite with tensile and zero mean load

M. AL-HUSSIEN[1], S. MALL[2,*] and J. R. CALCATERRA[1]

[1] *Department of Aeronautics and Astronautics, Air Force Institute of Technology, USA*
[2] *Materials and Manufacturing Directorate, Air Force Research Laboratory, AFIT/ENY, 2950 P. St., Bldg. 640, Wright-Patterson Air Force Base, OH 45433, USA*

Received 31 March 2000; accepted 31 October 2000

Abstract—This study characterized a woven fabric reinforced ceramic matrix composite, Nextel™ 312/Blackglas™, under monotonic and fatigue loading conditions at room and elevated (760°C) temperatures in order: (1) to investigate monotonic tensile and compressive loading behavior at room and elevated temperatures, (2) to establish the fatigue life diagrams (S–N curves) with tensile and zero mean load under low frequency (0.1 Hz) cycling condition at room and elevated temperatures, and (3) to investigate damage mechanisms and failure modes under monotonic and fatigue loading conditions. Fatigue lives under tension–compression cycling were much longer than those under tension–tension cycling at a given stress range for both room and elevated temperatures. However, fatigue lives under tension–compression cycling were much shorter than those under tension–tension cycling for a given maximum stress level at room temperature, but lives were about equal under these two loading conditions for a given maximum stress level at elevated temperatures. Further, fatigue lives were much shorter at elevated temperature than their counterparts at room temperature for a given stress range or for a given maximum stress level under the both tension–tension and tension–compression cycling conditions.

Keywords: Ceramic matrix composites; 2D woven composite; monotonic loading; fatigue loading; tension–compression cycling; room and elevated temperatures.

1. INTRODUCTION

Fiber/fabric reinforced ceramic matrix composites (CMCs) have the tremendous potential of application in various components in internal combustion engines, gas turbine engines, space vehicle engines and nozzles, etc. because of their capability to provide the higher damage tolerance and better oxidation resistance at elevated temperature with a considerable weight savings. While CMCs are relatively new

*To whom correspondence be addressed. E-mail: Shankar.Mall@afit.edu

materials, nevertheless several studies have been completed to investigate their behavior under various loading environments. Non-woven (i.e. fiber reinforced) CMCs have received a lot of attention in the recent past, and their behavior has been characterized extensively and reported (e.g. see References [1–5]). On the other hand relatively, a lot less work has been reported on woven (i.e. fabric reinforced) CMCs, their behavior needs to be therefore investigated further. Additionally, most of the research involving mechanical behavior characterization of the woven CMCs have been concentrated on tensile monotonic loading and tension–tension fatigue behavior (i.e. with a tensile mean load) (e.g. see References [6–14]).

During application of woven CMCs, which would take advantage of their higher damage tolerance and temperature capabilities, there would be many situations where these materials will be subjected to loading environments containing compressive loads. It is necessary, therefore, to investigate the mechanical behavior of CMCs under these loading environments as well before they are put into real use. Thus, this study investigated the mechanical behavior of a two-dimensional woven CMC under tensile and compressive monotonic loads as well as under tension–tension (i.e. with a non-zero tensile load) and tension–compression (i.e. with zero tensile load) cycling conditions at room and elevated temperatures, as a first step in this direction.

2. EXPERIMENTS

The material tested was Nextel™ 312/Blackglas™ woven fabric ceramic matrix composite (CMC). The Nextel 312, fabric reinforcement used in this CMC, is a commercially available polycrystalline metal oxide ceramic fiber. The reinforcement is made from alumina–boria–silica fibers, and has a composition of 62% $A1_2O_3$, 24% SiO_2, and 14% B_2O_3 (percentage by weight) [15]. Nextel™ 312 has a fiber diameter of about 10 microns, possesses desirable density and coefficient of thermal expansion, and is known for its thermomechanical qualities of retaining its strength at high temperatures for extended periods of time. The fabric reinforcement, Nextel 312 used in this study, was in the form of a five-harness satin weave cloth using 900 denier tows.

The Blackglas™ ceramic, used as matrix material in CMC of this study, is a silicon carboxide (SiC_xO_y), a highly refractory silicon-based glass containing 15–30%, atomically distributed carbon. This material is made from polymer precursor through a polymerization/pyrolyzation process. Blackglas™ has the advantages of resistance to oxidation, low density, very low viscosity, controllable thermal expansion coefficient by varying the carbon content, short cure time, no evolution of harmful reaction gases during the cure process, and ease as well as low cost of fabrication [15]. The CMC system used in this study was manufactured by using a low cost manufacturing procedure, and for proprietary reasons, the details are not known. A patented technique was used to prepare the *in-situ* boron nitride

coating (BN) on Nextel™ 312 ceramic fibers. The tested composite contained about 45% fiber volume fraction with about 10% porosity.

The CMC material was received in the form of specimens, which were rectangular in shape and had the nominal length, width, and thickness of 152, 12.3, and 2.3 mm, respectively. For monotonic tension and tension–tension fatigue tests, length of the specimen between the grips was 100 mm. However, specimens used for monotonic compressive and tension–compression fatigue tests were machined to reduce their length to 114 mm, and length of specimens between the grips was equal to 38 mm. This length was selected because it was short enough to alleviate flexure during the compression part of the testing. Thermocouple wires were attached on each side of the specimen to control the elevated test temperature of 760°C. These thermocouples were placed at 12.7 mm from the center of the specimen on both sides of specimens, so that uniform temperature distribution was obtained throughout the gage length of 25.4 mm.

A servohydraulic test machine was used in the present study. The hydraulic wedge grips of the test system were cooled using cold water. Cooling water was also used to cool the fixture containing the quartz heat lamps which was used to heat the specimen at 760°C in air. This test temperature was selected because of the anticipated use of Nextel™ 312/Blackglas™ up to this temperature in the real applications. Temperature controllers regulated the heat lamps to maintain the desired temperature of test section (of about 25.4 mm length) at 760°C. A high temperature extensometer with gage length of 12.7 mm was used to measure strain in the specimen.

The loading waveform in fatigue tests was of a triangular shape with a frequency of 0.1 Hz. The ratio of minimum to maximum stress levels ($\sigma_{\min}/\sigma_{\max}$), i.e. R-ratio in the tension–tension (T-T) and tension–compression (T-C) fatigue tests was 0.05 and -1, respectively. The $\sigma_{\min}$ is the smallest positive stress for T-T tests or the magnitude of the largest negative stress for T-C tests. The $\sigma_{\max}$ is the largest positive for both T-T and T-C tests.

3. RESULTS AND DISCUSSION

3.1. Monotonic tests

Table 1 shows the summary of all results from monotonic tension and compression tests. This table provides the average of maximum stress and maximum strain at failure, the proportional limit (PL), and Young's modulus of elasticity, E, obtained in this study. These average values are from three specimens and their variations over these specimens were less than $\pm 12\%$. Moduli of elasticity, obtained from the monotonic tension and compression tests, agreed with each other at both room and elevated temperatures. The room temperature value of Young's modulus from the present study is within 5% of the previously reported value from a similar CMC system [14].

Table 1.
Monotonic loading test results

Test type	Average strength (MPa)	Average failure strain %	Average Young's modulus (GPa)	Average proportional limit (MPa)
Room temp. tension	69	0.13	63	44
Elevated temp. tension	65	0.25	58	24
Room temp. compression	274	0.43	63	274
Elevated temp. compression	334	0.54	61	334

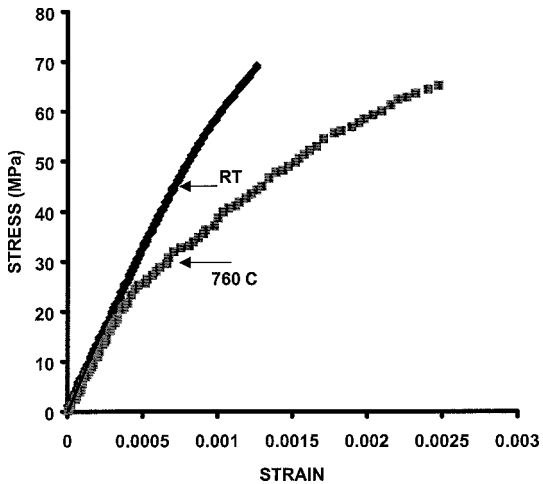

Figure 1. Monotonic tensile stress–strain relationship.

Typical stress–strain relationships from monotonic tensile test at room and elevated temperatures are shown in Fig. 1. It can be seen that the stress–strain relationship at the elevated temperature is linear up to about 25 MPa, which is the proportional limit; thereafter the curve showed the nonlinear behavior over a short strain region, and then the behavior is again almost linear before failure. This nonlinear behavior over the short strain region occurred possibly due to the matrix cracking, which is usually the source for the reduction in modulus of the fiber/fabric reinforced composites. The average Young's modulus of elasticity calculated from the linear region up to the proportional limit is 58 GPa, and the average slope in the nonlinear region is about 23 GPa. The stress–strain relationship from monotonic tensile test at room temperature showed similar nonlinear behavior. However, the change in the modulus before and after proportional limit is considerably less than its counterpart at elevated temperature showing that the matrix cracking-induced damage was considerably less at room temperature. The average failure stress at elevated temperature was about 65 MPa, which was slightly lower than the room temperature value of 69 MPa.

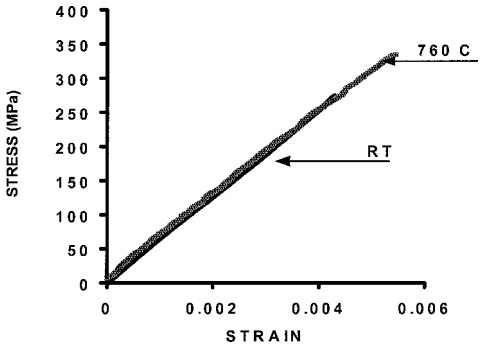

Figure 2. Monotonic compressive stress–strain relationship.

The average failure strains at room and elevated temperatures were 0.13% and 0.25%, respectively. Similar behavior (i.e. increase in the failure strain at the elevated temperature) has been observed also in the previous studies (e.g. see Ref. [16]). This difference in failure strains can be attributed to residual stresses in the tested composite. The elevated test temperature was very close to the final processing temperature of the tested CMC, i.e. the final furnace pyrolyzation temperature. Thus, the tested composite was almost stress free at the elevated test temperature. However, the composite develops the residual stress during the cool down phase of processing due to the thermal mismatch between fibers and matrix, which would pre-stress fibers in tension at room temperature. The residual stress can be approximately estimated from the difference in the failure strain at elevated and room temperatures (~0.12%) times the modulus (~60 GPa), i.e. about 72 MPa. However, it should be noted that the stress free condition at the elevated temperature did not help to increase the tensile strength of the composite due to increased damage at the elevated temperature, as depicted by the reduction in the modulus in stress–strain relationship beyond the proportional limit (see Fig. 1).

The typical stress–strain relationships under the compression monotonic test at both room and elevated temperatures were linear up to failure, as shown typically in Fig. 2. The average compressive strength at elevated temperature was 334 MPa, and the average failure strain was 0.55%, while their counterparts were 274 MPa and 0.43% respectively at room temperature. The Young's modulus of elasticity at both temperatures is of same value, i.e. about 61 GPa. The comparison between these room and elevated temperature tests shows that the compressive strength at room temperature was about 60 MPa less than that at the elevated temperature, and the failure strain at room temperature is about 0.11% less than that at the elevated temperature, which is somewhat unexpected. However, this can be explained if the role of the residual stress is accounted. As mentioned earlier, the residual tensile stress and strain in the fibers of the tested composite are estimated about 72 MPa and 0.12%, respectively, which are almost equal to the difference in compressive strength and failure strain values at room and elevated temperatures.

The preceding discussion about the role of the residual stresses on the differences between the failure strains and strength at room and elevated temperatures under the monotonic tensile and compressive loadings is no doubt a very simplistic explanation if one considers the complexity in the deformation and damage mechanisms involved in the fabric reinforced ceramic composites. These may be matrix cracking, fiber/matrix debonding, interfacial shear stress and fiber breakage. The role of these factors in the fiber reinforced ceramics matrix composites are very well documented in the literature (e.g. see Ref. [1]). However, there is minimal understanding at present about these factors in the fabric reinforced ceramics matrix composites, especially when these composites exhibit almost bilinear stress–strain behavior as in the present study (or in Ref. [16]) where there appears to be no change in the matrix cracking density with increasing load or with cycling. Further, it is an extremely challenging experimental task to track the development of matrix cracking during testing of fabric reinforced ceramics matrix composites tests and to distinguish these from the preexisting one before testing which is very common in most of these composites.

3.2. Fatigue tests

The fatigue behavior of the tested woven CMC system was characterized by the applied stress (S) versus fatigue life (N) relationship, i.e. $S-N$ curve, macroscopic behavior involving the strain response during cycling, and microscopic evaluation of damage and failure mechanisms. These will be discussed in the following.

3.2.1. Fatigue life. The measured fatigue lives from both T-T and T-C cycling conditions at room and elevated temperatures will be compared on the basis of stress range and maximum stress in this section. Figure 3a shows the comparison of fatigue lives for both T-T and T-C fatigue loadings, with tensile and zero mean loads respectively, at room and elevated (760°C) temperatures on the stress range basis. On the comparison of fatigue lives ($S-N$ curves) for two fatigue conditions: T-T and T-C at both temperatures, it can be seen that the T-C fatigue lives are much longer than the T-T fatigue lives for a given stress range. This can be attributed to the effects of the mean stress. As commonly known in the fatigue literature, the mean stress can have a substantial influence on the fatigue behavior, with tensile mean stress being detrimental to fatigue life. Thus, the tensile mean stress present in the T-T case appears to have had an adverse effect on the fatigue lives as compared to that under the T-C case, at both room and elevated (760°C) temperatures.

For both T-T and T-C cycling conditions, fatigue lives are much shorter at elevated temperature than their counterparts at room temperature for a given stress range. This clearly demonstrates the effects of exposure to the elevated temperature on the fatigue lives of the tested CMC system. As is well known in CMCs literature, exposure to the temperature in oxygen-rich environments (i.e. the laboratory conditions in present study) weaken the fibers and matrix–fiber interface, which results in the significant decrease in the fatigue life and/or damage tolerance

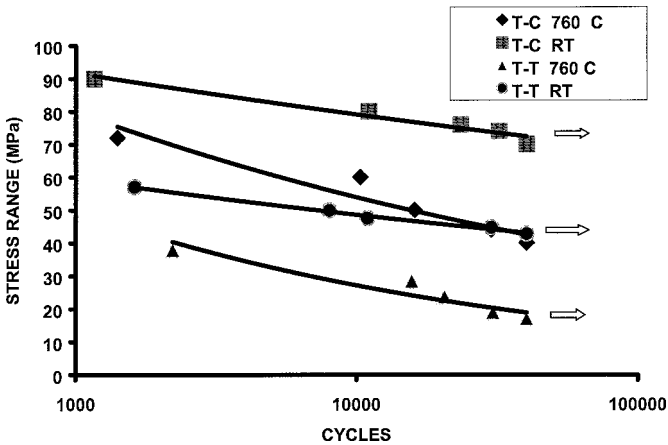

Figure 3a. Fatigue life diagram based on stress range.

of the CMC. As can be seen in Fig. 3a, the tension–tension cycling condition at the elevated temperature had the shortest fatigue lives. Another physical effect of the tensile mean stress is that any existing cracks T-T cycling specimen will remain open throughout the fatigue cycle. In contrast, cracks in T-C specimen with zero mean stress will be subjected to closure for at least half portion of the fatigue cycle. Thus, damage induced oxidation effects would be greater in the T-T case, thereby reducing the T-T fatigue life in comparison to T-C fatigue life at the same stress range.

Figure 3b shows the comparison of fatigue lives for both T-T and T-C fatigue loadings at room and elevated (760°C) temperatures on the basis of applied maximum stress. As can be seen here, fatigue lives under T-C cycling were much shorter than those under T-T cycling for a given maximum stress level at room temperature. This again demonstrates the previous observation that the tensile mean stress present in the T-T case appears to have had an adverse effect on the fatigue lives as compared to that under the T-C case with zero mean stress, or the presence of the compressive portion of applied cyclic loading has the detrimental effects on the fatigue damage introduced during the tensile portion of the cyclic loading. However, fatigue lives were about equal under these two loading conditions for a given maximum stress level at elevated temperature. This shows that the maximum stress, which is the same in both cases in spite of different stress range, is the governing parameter for fatigue damage or fatigue life as in the case of creep response of ceramics and ceramics composites [1, 7, 8, 16]. Furthermore, fatigue lives were much shorter at elevated temperature than their counterparts at room temperature for a given maximum stress level under the both T-T and T-C cycling conditions which clearly reiterates the effects of exposure to the elevated temperature on the tested fatigue life as discussed previously.

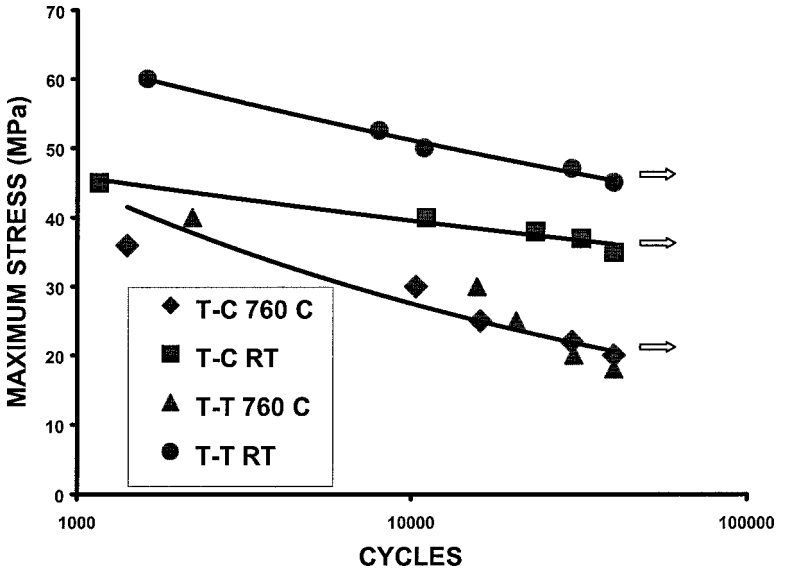

Figure 3b. Fatigue life diagram based on maximum stress.

3.2.2. Macroscopic response. Macroscopic response in terms of stress–strain hysteresis was monitored during fatigue tests. The stress–strain hysteresis loops were of the closed form with zero width and of linear shape after few initial cycles, but there was variation in the maximum and minimum strains during cycling in some cases as discussed in the following, i.e. the shift of these loops without any S-shaped behavior which is the characteristic of interfacial shear stress at the fiber/matrix interface during loading and unloading [17]. Further, the absence of any non-linearity in these loops further indicates minimal growth of matrix cracks or total lack of it except for the initial development of matrix crack over first few cycles when loaded beyond the proportional limit which is also indicated by almost bilinear behavior of monotonic stress–strain relationship (Fig. 1).

Hence the maximum and minimum strains will be discussed here to interpret the damage behavior of the tested composite. There was practically no variation in both maximum and minimum strain values from the onset of cycling until failure in T-T fatigue tests at room temperature. This suggested that either no or a very little damage in the form of matrix cracking or degradation of fiber/matrix interfacial shear stress occurred in the tested CMC, except for relative motion between fiber bundles during cycling which could not be discerned from the macroscopic response in this case. On the other hand, Fig. 4 shows the typical variation of maximum and minimum strains in T-T fatigue test at elevated temperature. In this case, maximum and minimum strains started at about 0.06% and 0.03%, respectively; and then both of these strains increased as the number of cycles progressed up to failure. However, the difference between maximum and minimum strains remained almost constant until near failure, where the difference increased slightly. This accumulation of

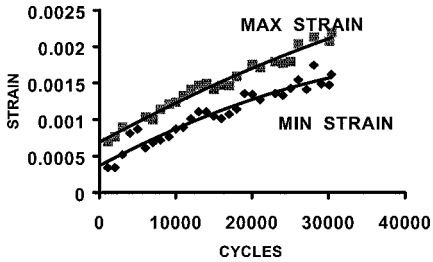

Figure 4. Typical history of strain during tension–tension cycling at elevated temperature (20 MPa).

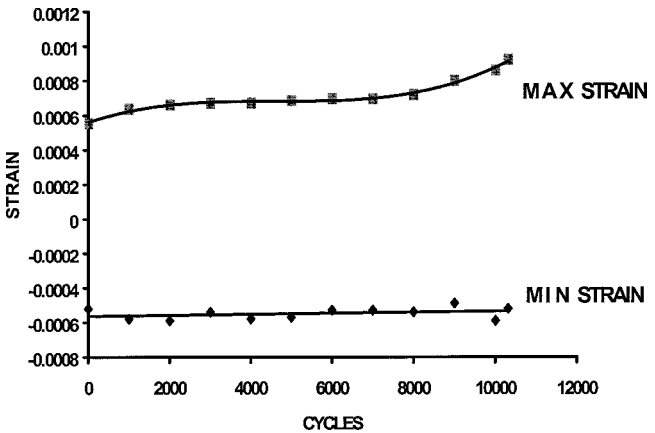

Figure 5. Typical history of strain during tension–compression cycling at elevated temperature (40 MPa).

strain without any noticeable increase in the modulus during most of the fatigue life indicates that the deformation mechanism seen by the composite during most of T-T cycling is predominantly from creep/ratcheting deformation. This can be attributed to effects of the positive mean stress at the elevated temperature, and its effects are also evident in the fatigue life diagram, especially when plotted on the basis of the applied maximum stress (Fig. 3b).

In T-C fatigue tests at room temperature, maximum and minimum strains remained almost constant from the beginning of the test up to failure. This again suggests that no damage or little damage in the form of matrix cracking or degradation of fiber/matrix interfacial shear stress occurred in the tested CMC except for relative motion between fiber bundles during cycling, which could not be discerned from the macroscopic response in this case. On the other hand, Fig. 5 shows the typical behavior of maximum and minimum strains during a T-C fatigue test at elevated temperature. As can be seen, the minimum strain did not vary much but remained almost constant. The maximum strain also remained constant for most of the fatigue life (about 80% of the fatigue life in this test), after which it increased with number of cycles until failure. This again shows that the fatigue damage occurred in this case predominantly from creep/ratcheting deformation, and the presence of com-

pressive minimum stress forced the minimum strain not to vary during cycling. This is again evident from the fatigue life diagram (Fig. 3b) when plotted on the basis of the applied maximum stress, where fatigue lives were about equal under T-T and T-C loading conditions for a given maximum stress level at elevated temperature.

In summary, the elevated temperature had no or a little effect on the strain behavior of the material under investigation when it was subjected to T-C fatigue cycling with zero mean stress. On the other hand, a noticeable difference was seen in the strain behavior of the tested CMC when it was subjected to T-T fatigue loads at elevated temperature. Under T-T fatigue condition at room temperature, both maximum and minimum strains remained almost constant up to failure; but these strains, at elevated temperature, increased at the same rate with the cycling, and the difference between them remained almost constant, indicating that creep/ratcheting occurred under T-T fatigue loading at elevated temperature condition due to the presence of the positive mean stress.

4. DAMAGE MECHANISMS

4.1. Monotonic tests

The damage in monotonic tensile tests, at both temperatures, initiated at the macropores in the warp (i.e. longitudinal or in the loading direction) and fill (i.e. transverse or perpendicular to loading direction) yarns. It was followed by matrix cracking, interface debonding of fibers, and fiber breaking, all these in the fill yarn, and then the eventual fiber breaking of fibers in the warp yarn. Overall comparison between room and elevated temperatures showed that the fracture surface in the elevated temperature tests had a slightly greater roughness than that in the room temperature tests due to the presence of relatively more fiber pull-out caused in the transverse yarn by elevated temperature. This comparison of fiber pull-out in the transverse yarn between room and elevated temperatures is shown in Fig. 6. As mentioned earlier, the reduction in the modulus beyond the proportional limit in the stress–strain at elevated temperature is considerably more than its counterpart at room temperature (see Fig. 1). Hence, this macroscopic difference between the monotonic tensile loading behaviors at two temperatures can be attributed to the localized matrix cracking at the proportional limit and debonding or weakening of the fiber/matrix interface due to relaxation of residual stress at elevated temperature.

The fracture surfaces in the monotonic compressive tests were similar in both room and elevated temperatures. These were considerably rougher in appearance in comparison to their counterparts in monotonic tensile tests due to the crushing of matrix, which was noticed in the form of powder that came out of the fractured surfaces. Further, delamination between the plies also occurred during compression, as shown typically in Fig. 7. Finally, in all of these monotonic tensile and compressive tests, the fracture occurred almost perpendicular to the applied load in the gage section of specimens.

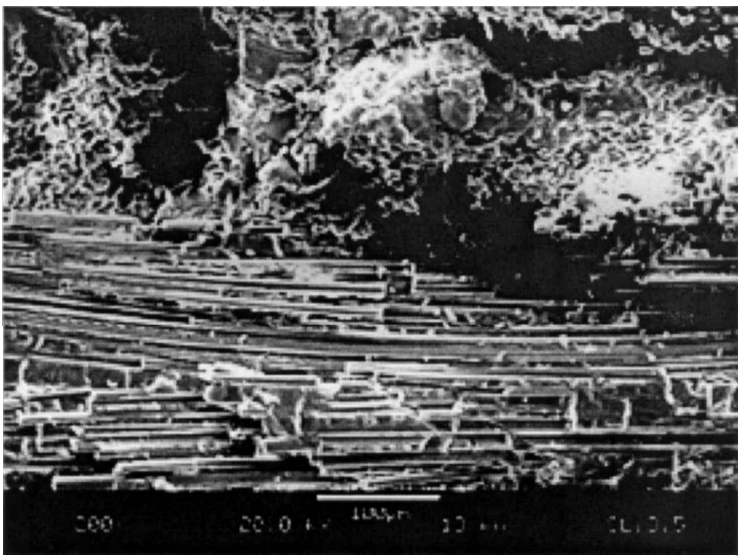

Figure 6a. Typical fracture surface, monotonic tension, room temperature, ×200.

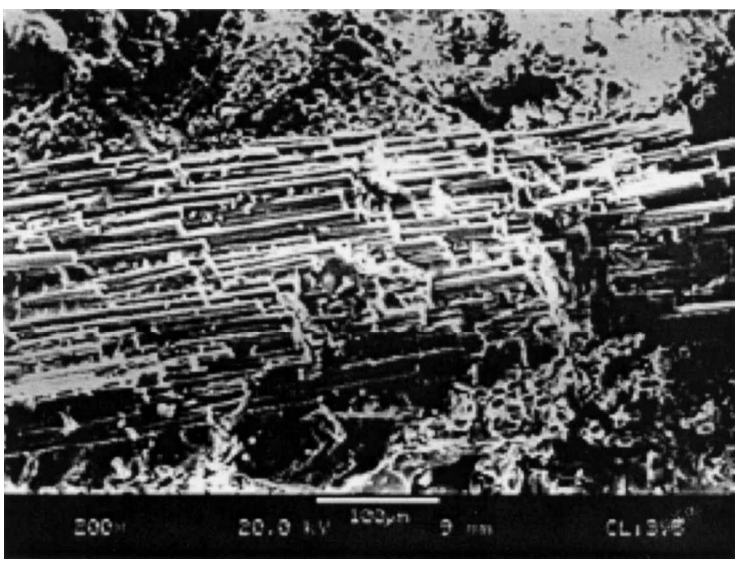

Figure 6b. Typical fracture surface, monotonic tension, elevated temperature, ×200.

4.2. Fatigue tests

The morphology of fracture surfaces of specimens tested under T-T fatigue at both temperatures was basically similar to its counterpart from monotonic tensile tests except that, in the case of fatigue tests, there were two distinct regions. These two regions clearly belonged to the damage development during cyclic loading by their slightly smoother appearance and to catastrophic failure from overloading once

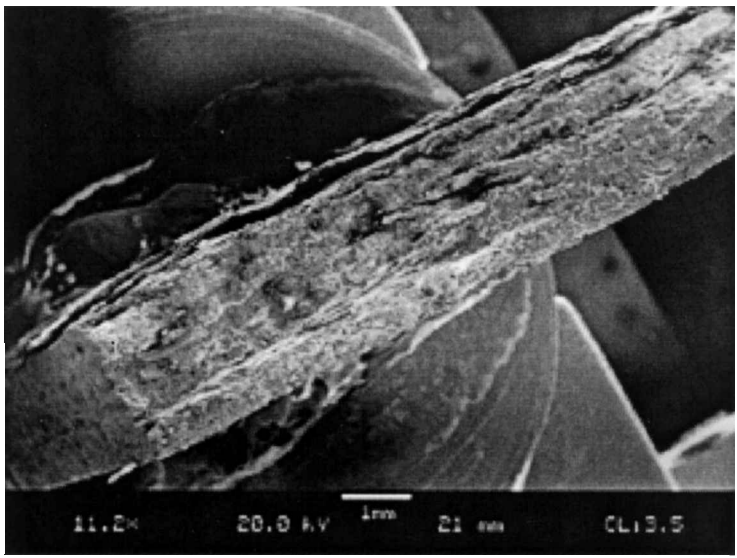

Figure 7. Typical fracture surface, monotonic compression at elevated temperature.

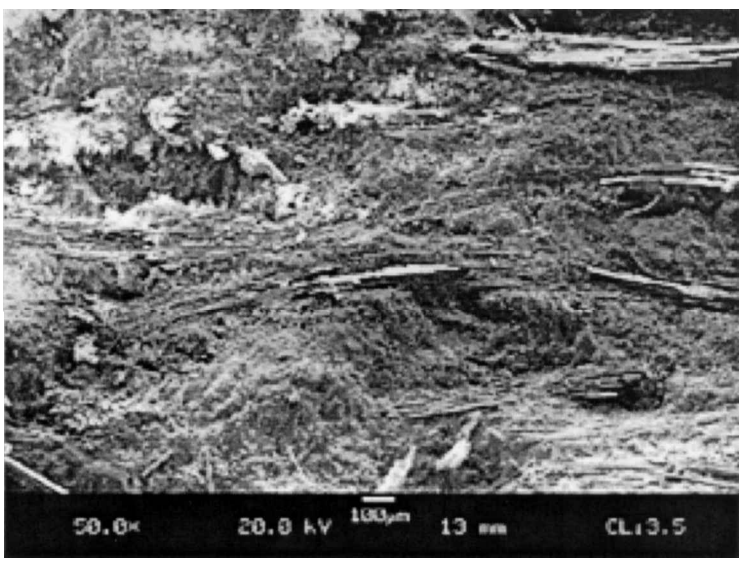

Figure 8a. Typical fracture surface, tension–tension fatigue at room temperature, ×50.

the remaining cross-section could not withstand the applied maximum load. The ratio of area of these two regions ranged from about 0.5 to 1.0 depending upon the applied maximum load. The fatigue damage, at both temperatures, initiated at the macropores in the warp (i.e. longitudinal or in the loading direction) and fill (i.e. transverse or perpendicular to loading direction) yarns. It was followed by matrix cracking, interface debonding of fibers, and fiber breaking, all in the fill

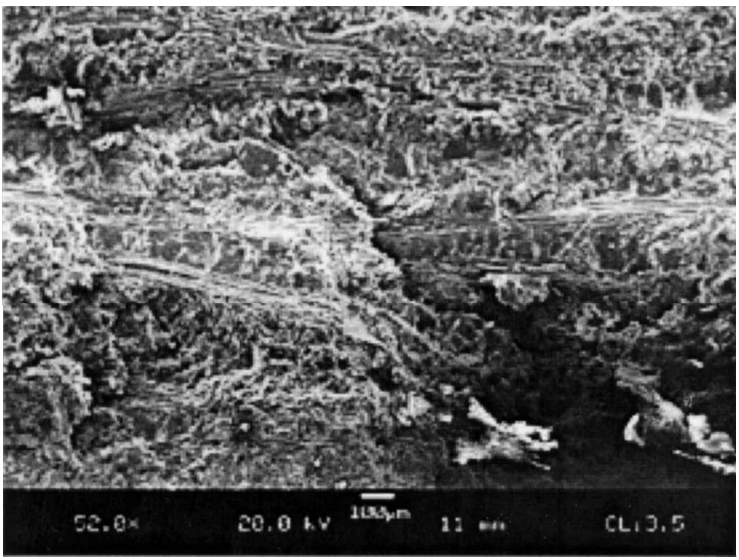

Figure 8b. Typical fracture surface, tension–tension fatigue at elevated temperature, ×50.

yarn, and then the eventual fiber breaking in the warp yarn. Overall comparison between room and elevated temperatures showed that the fracture surface in the elevated temperature tests had a slightly greater roughness than that in the room temperature test due to the presence of more fiber pull-out caused in the transverse yarn at elevated temperature. This occurred due to debonding of fibers followed by matrix cracking at many planes due to weaker matrix–fiber interface as a result of relaxation of the residual stresses from the exposure to elevated temperature, while it occurred at one plane in room temperature tests, as shown in Fig. 8.

The morphology of fracture surfaces of specimens tested under T-C fatigue at both temperatures was basically similar to its counterpart from tension–tension tests, which clearly indicates that the tension part of T-C fatigue was the main contributor towards the failure. This is also apparent from the S–N relationship as discussed earlier.

5. CONCLUSIONS

This study investigated the monotonic tension and compression loading, and the tension–tension and tension–compression fatigue behavior of a two-dimensional woven ceramics matrix composite at room temperature and 760°C. The ultimate strength at the elevated temperature was almost equal to that at the room temperature under monotonic tensile loading, and it was higher in the compressive monotonic loading at the elevated temperature than its counterpart at the room temperature. This behavior could be explained from the effects of residual stresses developed during processing of CMCs and effects of elevated temperature. There was no effect on the Young's modulus due to temperature change and loading mode.

Fatigue lives under tension–compression cycling were much longer than those under tension–tension cycling at a given stress range for both room and elevated temperatures. However, fatigue lives under tension–compression cycling were much shorter than the counterpart under tension–tension cycling for a given maximum stress level at room temperature, but fatigue lives were about equal under these two loading conditions for a given maximum stress level at elevated temperatures. Further, fatigue lives were much shorter at elevated temperature than their counterparts at room temperature for a given stress range or for a given maximum stress level under the both tension–tension and tension–compression cycling conditions.

Acknowledgements

The support of this study by the Air Force Office of Scientific Research (Dr. H. Thomas Hahn) is gratefully acknowledged.

REFERENCES

1. A. G. Evans and F. W. Zok, The physics and mechanics of fiber-reinforced brittle matrix composites, *J. Mater. Sci.* **29**, 3857–3896 (1994).
2. S. Mall and R. Y. Kim, Failure mechanisms in laminates of silicon carbide/calcium aluminosilicate ceramic composite, *Composites* **23** (4), 215–222 (1992).
3. F. A. Opalski and S. Mall, Tension–compression fatigue behavior of a silicon carbide calcium-alumino-silicate ceramic matrix composites, *J. Reinforced Plast. Compos.* **13**, 420–438 (1994).
4. A. Rodrigues, G. A. Rosa and M. Steen, Fatigue behavior of a ceramic matrix composite, 2D C_{fiber}/SiC_{matrix}, *J. Amer. Ceramic Soc.* **57**, 351–356 (1995).
5. S. F. Shuler, J. Holmes and X. Wu, Influence of loading frequency on the room-temperature fatigue of a carbon-fiber/SiC-matrix composite, *J. Amer. Ceramic Soc.* **76** (9), 2327–2336 (1993).
6. N. Chawla, Y. K. Tur, J. W. Holmes and J. R. Barber, High frequency fatigue behavior of woven fiber reinforced polymer derived ceramics matrix composites, *J. Amer. Ceramics Soc.* **81** (5), 1221–1230 (1998).
7. S. Zhu, M. Mizuno, Y. Nagano, J. Cao, Y. Kagawa and H. Kaya, Creep and fatigue behavior in an enhanced SiC/SiC composite at high temperature, *J. Amer. Ceramics Soc.* **81** (5), 2269–2277 (1998).
8. S. Zhu, M. Mizuno, Y. Nagano, J. Cao, Y. Kagawa and H. Kaya, Creep and fatigue behavior in Hi-Nicalon fiber reinforced silicon carbide composite at high temperatures, *J. Amer. Ceramics Soc.* **82** (1), 117–128 (1999).
9. J. C. McNuty and F. W. Zok, Low cycle fatigue of Nicalon fiber reinforced ceramic composites, *Compos. Sci. Technol.* **59**, 1597–1607 (1999).
10. G. Camus, L. Guillaumat and S. Baste, Development of damage in a 2D woven C/SiC composite under mechanical loading: I. Mechanical characterization, *Compos. Sci. Technol.* **56**, 1363–1372 (1996).
11. S. S. Campbel and S. T. Gonczy, In-situ formation of boron nitride interfaces on Nextel 312™/BlackGlas™ continuous ceramic fiber I: Nitriding process and BlackGlas™ ceramic matrix composite properties, *Ceramic Engng Sci. Proc.* **15** (4), 327–336 (1994).

12. S. S. Campbel and S. T. Gonczy, In-situ formation of boron nitride interfaces on Nextel 312™/BlackGlas™ continuous ceramic fiber I: Oxidation of BlackGlas™ ceramic matrix composite, *Ceramic Engng Sci. Proc.* **15** (4), 337–343 (1994).
13. K. R. Vaidyanathan, W. R. Cannon, S. Danforth, A. G. Tobin and J. Holmes, Effect of oxidation on the mechanical properties of Nextel 312™/BN/BlackGlas™, *Materials Research Society Symposium Proceedings* **365**, 429–434 (1995).
14. K. R. Vaidyanathan, J. Sankar and A. D. Kelkar, Mechanical properties of Nextel 312™ fiber-reinforced SIC matrix composites in tension, *Ceramic Engng Sci. Proc.* **15** (4), 251–261 (1994).
15. M. N. G. Nijhad and J. K. Bayliss, Processing and performance of continuous fiber ceramic composites using vacuum assisted resin transfer molding and BlackGlas™ preceramic polymer pyrolysis, *Ceramic Engng Sci. Proc.* **18** (3), 391–399 (1997).
16. S. S. Lee, L. R. Zawada, J. M. Staehler and C. A. Falsom, Mechanical behavior and high temperature performance of a woven Nicalon/Si-N-C ceramic matrix composite, *J. Amer. Ceramics Soc.* **81** (7), 1797–1811 (1998).
17. B. Yang and S. Mall, Modeling of stress–strain hysteresis behavior in brittle matrix composites under cyclic loading, in: *Proc. Intern. Conf. Computing and Science '2002*, University of California at Los Angeles, Los Angeles, CA, USA (2000).